Multichannel thermal transport in crystalline Tl$_3$VSe$_4$

Ankit Jain[*]

Mechanical Engineering Department, IIT Bombay, Mumbai 400076, India

The validity of the particlelike phonon picture in describing the thermal transport physics in strongly anharmonic crystalline materials is a subject of recent debate. On the one hand, the Peierls-Boltzmann transport equation-based particlelike treatment of phonons was found to be insufficient in explaining the experimentally observed ultralow thermal conductivity of Tl$_3$VSe$_4$, and subsequently another thermal transport theory based on an additional thermal transport channel was proposed. On the other hand, the validity of this multichannel transport was questioned through a higher-level theory accounting for higher-order terms. Here, using the highest level of thermal transport theory with contributions from a temperature-dependent potential energy surface, lattice thermal expansion, force constant renormalization, long-range Coulombic interactions, and higher-order quartic phonon scattering processes, the validity of multichannel thermal transport is tested for Tl$_3$VSe$_4$. The particlelike transport channel is found to severely underpredict the experimentally measured thermal conductivity by a factor of 3 at a temperature of 300 K. The contribution of the wavelike coherent transport channel is found to be twice that of the particlelike channel, and the total thermal conductivity from multichannel transport theory is found to be in agreement with experimental measurements.

The understanding of thermal transport physics in low thermal conductivity crystalline materials is of great importance for applications such as thermoelectric energy conversion, thermal barrier coatings, data storage, and nuclear reactors [1–3]. Conventionally, the thermal transport in crystalline materials is described by the Peierls-Boltzmann transport equation (PBTE) using well-defined phonon modes [4,5]. This phononic thermal transport from PBTE, however, was recently found to be insufficient in explaining the experimentally observed ultralow thermal conductivity of the body-centered-cubic crystalline material Tl$_3$VSe$_4$ [6]. At a temperature of 300 K, by solving PBTE, Mukhopadhyay *et al.* [6] obtained a phonon thermal conductivity of 0.16 W/mK, which was only one-half of their experimentally measured value (0.30 ± 0.05 W/mK). In solving PBTE, the authors found modes with mean free paths less than the interatomic distances, which questions the validity of the phonon picture. To explain the experimental findings, the authors proposed a phenomenological two-channel thermal transport model whereby long mean free path modes were described by a standard phonon channel using PBTE whereas small mean free path modes were described by a hopping/coherent channel using Einstein's or Cahill's model [7,8].

Inspired by the above shortcoming of PBTE in describing thermal transport in strongly anharmonic crystalline materials, Simoncelli *et al.* [9] derived a transport equation based on the phonon velocity operator. The diagonal and off-diagonal elements of the proposed velocity operator describe the particlelike propagation of phonons and wavelike interbranch tunneling of coherence (diffusons and locons), respectively.

Using this model, the authors were able to explain the glasslike thermal transport in CsPbBr$_3$, perfectly in agreement with experiments. Subsequently, a vibrational hierarchy-based phenomenological dual-phonon transport model was also proposed recently by Luo *et al.* [10] to explain the experimentally observed thermal conductivity of La$_2$Zr$_2$O$_7$.

In all of the above studies, the validity of the proposed multichannel models was tested by solving PBTE using the lowest-order theory employing only cubic anharmonicity. This approximation was put to the test recently for Tl$_3$VSe$_4$ by Xia *et al.* [11]. The authors concluded that the underprediction of thermal conductivity in the study of Mukhopadhyay *et al.* [6] was due to the use of the lowest-order anharmonicity in the transport theory. With the introduction of higher-order anharmonicity, phonon modes renormalized, causing more than a factor of 2 increase in the thermal conductivity. The resultant thermal conductivity is in perfect agreement with experiments without the need for an additional wavelike coherent transport channel, thus challenging the validity of the proposed multichannel thermal transport models.

The increase in thermal conductivity with higher-order anharmonicity in the study of Xia *et al.* [11] is counterintuitive. Nevertheless, the validity of the multichannel transport model remains an outstanding unresolved question and requires further independent investigation.

In this Rapid Communication, the validity of the multichannel thermal transport model is tested for Tl$_3$VSe$_4$ using the highest-accuracy thermal transport theory to date including the effects of a temperature-dependent potential energy surface (PES), lattice thermal expansion, self-consistent phonon renormalization, higher-order four-phonon scattering, longitudinal optic (LO)-transverse optical (TO) splitting, an iterative/full solution of PBTE, and multichannel

---

thermal transport. The predicted thermal conductivity from the highest-order theory with only a particlelike phonon thermal transport channel is found to fall short of the experimentally measured value by more than a factor of 2. The contribution of the coherent channel is more than that of the particlelike channel, and the total thermal conductivity obtained from the two-channel thermal transport model is in perfect agreement with the experimental measurements.

At the lowest level of theory, the phonon thermal conductivity is obtained from PBTE using the relaxation time approximation (RTA) with lowest-order cubic anharmonicity and quasiharmonic approximation-based interatomic force constants (IFCs) [12]. At this level of theory, the atoms are assumed to occupy their 0-K equilibrium positions and the scattering is considered only through three-phonon (3-ph) processes. The thermal expansion, the renormalization of phonons due to anharmonicity, and the higher-order anharmonicity in phonon scattering are ignored at this level of theory. The improvements in thermal transport theory beyond this lowest-order approximation are obtained through the temperature-dependent sampling of PES, IFC renormalization, higher-order ph-ph scattering, full solution of PBTE, and multichannels for thermal transport, and are presented in Fig. 2(a). The effect of temperature-dependent PES and lattice thermal expansion in the extraction of IFCs is included by sampling atomic configurations from *ab initio* molecular dynamics simulations or a stochastic thermal sampling technique [13–15]. The sampled configurations from molecular dynamic simulations correspond to classical statistics, whereas both classical or quantum statistics are possible through stochastic thermal sampling [16]. The second-order anharmonicity is considered by including quartic IFCs and self-consistently correcting harmonic and/or cubic/quartic IFCs for second-order effects [17,18]. The second-order anharmonicity is included in phonon scattering through four-phonon (4-ph) scattering processes. Finally, the full solution of the PBTE is obtained by solving the PBTE iteratively [19,20] and the effect of multichannel thermal transport is included by considering both particle- and wavelike thermal transport channels [9]. Further details on the implementation and computational aspects of these theories are presented in the Supplemental Material (SM) (see Sec. S1) [21–26].

The effect of different levels of theory on the obtained phonon dispersion is presented in Fig. 1. The phonon dispersion and atom-decomposed density of states of Tl_3VSe_4 obtained by considering temperature-dependent PES, IFC renormalization, and lattice thermal expansion are reported in Fig. 1(a). The effect of temperature is maximum for acoustic phonons at the H-symmetry point of the Brillouin zone. With increasing temperature, these modes become stiff by up to a factor of 2 at a temperature of 300 K. These modes have a majority contribution from heavy Tl atoms [see the atom-decomposed partial density of states in Fig. 1(a)] and behave similar to the rattlerlike modes of caged compounds [27]. The rattling motion of these modes is also reflected in their small participation ratio, as reported in Fig. S3(a). The strong temperature-dependent stiffening of these Tl-dominated modes is due to the associated large mean-square atomic displacements of Tl atoms as reported in Fig. S2.
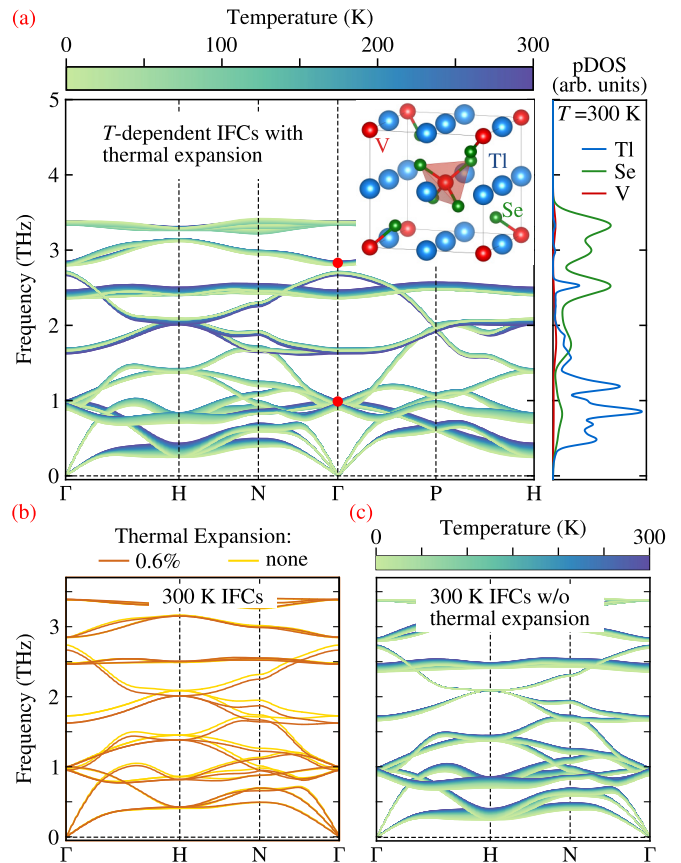

FIG. 1. The phonon dispersions of Tl_3VSe_4 obtained using (a) temperature-dependent sampling of PES with thermal expansion, (b) 300-K PES with and without thermal expansion, and (c) 300-K PES without thermal expansion. The red solid symbols in (a) denote the experimentally measured Raman-active modes from Ref. [6]. The atom-decomposed partial density of states at a temperature of 300 K is also shown in (a). The 0.6% thermal expansion in (b) corresponds to experimental measurements at a temperature of 300 K.

Other than low-lying modes, the optical phonon band at 2.5 THz also has a significant contribution from loosely bound Tl atoms. Similar to low-frequency modes, with increasing temperature, these modes also undergo strong renormalization resulting in stiffened frequencies. In contrast, for modes with no or a negligible contribution of Tl atoms, frequency softening is observed with increasing temperature. This softening is due to lattice thermal expansion, as presented in Fig. 1(b).

The temperature-dependent phonon dispersion presented in Fig. 1(a) is both qualitatively and quantitatively different than that reported by Xia *et al.* [11]. Noticeably, the authors predicted stiffening of all modes in the entire Brillouin zone with frequencies lower than 5 THz. In the present study, while stiffening is observed for modes with a sizable Tl contribution, softening is observed for all other modes with a negligible Tl contribution. The results reported by Xia *et al.* [11] are reproduced here by considering only IFC renormalization, i.e., by ignoring contributions from the lattice thermal expansion and temperature-dependent PES in Fig. 1(c). The role of lattice thermal expansion and temperature-dependent PES are highlighted in Figs. 1(b) and S4, respectively. The
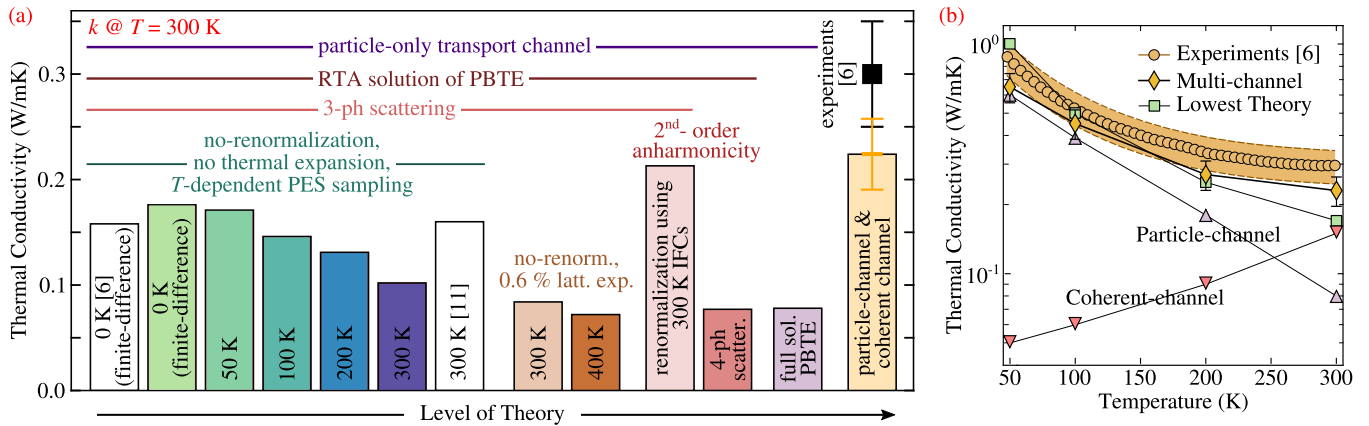
FIG. 2. (a) The 300-K and (b) temperature-dependent thermal conductivity of Tl_3VSe_4 as predicted from different levels of theory. In (a) the values reported by Mukhopadhyay *et al.* [6] and Xia *et al.* [11] are also positioned on the theory axis and are distinguished using the open bars. The prediction error bars correspond to 15% uncertainty arising from the choice of the exchange-correlation functional [6,28].

phonon dispersion in Fig. 1(c) is obtained using 300-K IFCs. These results suggest that (i) ignoring lattice thermal expansion erroneously causes the stiffening of non-Tl modes with temperature and (ii) the use of strongly anharmonic 300-K IFCs to renormalize harmonic frequencies at 50 K causes overstiffening of the modes.

Now that the importance of lattice thermal expansion and temperature-dependent IFCs is established for harmonic properties, their effect is next tested on the predicted thermal conductivity of Tl_3VSe_4 in Fig. 2(a). The reported thermal conductivities in Fig. 2(a) are for a temperature of 300 K (i.e., phonon occupations and scattering rates are obtained at a temperature of 300 K) though PES sampling/IFC renormalization are performed at different temperatures as reported in the figure.

The thermal conductivity predicted from the lowest level of theory using 0-K PES sampling to extract IFCs using the finite difference of forces, without renormalization, and employing only 3-ph processes for ph-ph scattering is 0.18 W/mK. This predicted thermal conductivity is in excellent agreement with the results of Mukhopadhyay *et al.* [6] and Luo *et al.* [10], though both of these literature results are obtained using a different set of computational tools (ShengBTE and VASP as opposed to in-house code and Quantum Espresso in this study [29]).

As discussed above for phonon dispersion, with the temperature-dependent sampling of the PES, the anharmonicity experienced by the atoms increases, resulting in a rise in the strength of anharmonic IFCs. The effect of this increased anharmonicity is minimal at low temperatures and the predicted thermal conductivity with 50-K IFCs is the same as that predicted using 0-K IFCs. With increasing temperature, however, the PES becomes strongly anharmonic and the thermal conductivity predicted using 300-K IFCs is up to 40% smaller than that predicted using finite-difference-based 0-K IFCs.

It is worthwhile mentioning here that this decrease in thermal conductivity with increasing anharmonicity as arising from the temperature-dependent sampling of PES is in contrast with the findings of Klarbring *et al.* [30] where the authors predicted the opposite trend. In their study, while extracting anharmonic IFCs from force-displacement data, the

authors first fitted only cubic IFCs followed by a subsequent fitting of quartic IFCs to the residual force displacement data. For Si, using this IFC extraction scheme, a similar trend suggesting an increase in thermal conductivity with a high-temperature sampling of PES is observed here (see Table S1). This fitting scheme is, however, not physical and depends, for instance, on the order of cubic/quartic IFC fitting. When both cubic and quartic IFCs are extracted simultaneously, a decrease in thermal conductivity is obtained with high-temperature sampling of the PES (Table S1).

The thermal conductivity reported by Xia *et al.* [11] at a temperature of 300 K using 300-K sampling of PES from a molecular dynamics simulation is 0.17 W/mK, which is the same as the values predicted using the 0-K sampling of PES in Refs. [6,10], thereby suggesting no effect of temperature-dependent sampling of PES for strongly anharmonic solid Tl_3VSe_4. This is in sharp contrast with Si, which is only mildly anharmonic and undergoes a 5% reduction in thermal conductivity at a temperature of 300 K with the inclusion of temperature-dependent IFCs (Table S1). For Tl_3VSe_4, the results of Xia *et al.* [11] are an overprediction by 60% compared to the results obtained in this work. This overprediction in the study of Xia *et al.* [11] could be due to (a) the use of a different exchange-correlation functional (see Refs. [6,28] for the effect of the exchange-correlation functional on thermal conductivity), (b) the use of classical Boltzmann statistics with coarse simulation parameters for the sampling of PES [16,31], (c) nonconvergence of IFCs with respect to the force-displacement data size [see Fig. S1(b)], and/or (d) non-inclusion of long-range forces arising from the Born effective charges in the PES sampling.

Moving up the theory level, the thermal conductivity decreased by 18% with a thermal expansion of 0.6% at a temperature of 300 K. As shown in Fig. 1(c), this decrease predominately originates from softening of the phonon modes and an associated reduction of group velocities with the lattice expansion.

For strongly anharmonic materials, it is required to renormalize bare IFCs for higher-order anharmonicity and include phonon-phonon scattering due to higher-order processes. The harmonic IFCs are renormalized using bare quartic IFCs and

the renormalized harmonic IFCs are in turn used to self-consistently correct the cubic and quartic IFCs. For Tl$_3$VSe$_4$ at a temperature of 300 K, this renormalization results in more than a factor of 2 increase in the thermal conductivity. On including second-order anharmonicity in phonon scattering through 4-ph scattering processes, however, the thermal conductivity reduces by more than a factor of 2, thereby offsetting the gain from IFC renormalization and bringing the value back to 0.08 W/mK. It is interesting to note that this cancellation of the contribution from renormalization and 4-ph scattering is similar to the findings of Ravichandran *et al.* [18].

Solving PBTE via a full solution has no effect on the predicted thermal conductivity for Tl$_3$VSe$_4$ at 300 K and the final contribution of particlelike propagating modes stands at 0.08 W/mK. This value falls short of experimental measurements by a factor of 3–4 and is not accountable by exchange-correlational functional-based computational uncertainties (10%–20%) or experimental errors (0.05 W/mK). Incidentally, the contribution of a wavelike coherent transport channel as obtained from the off-diagonal component of the velocity operator [9] is 0.15 W/mK, and thus bringing the total contribution from two-transport channels to within the uncertainty range of the experimentally measured value of 0.30 W/mK.

To further confirm the validity of the multichannel transport, the thermal conductivity obtained using the highest level of theory is plotted as a function of temperature and compared against experimental measurements in Fig. 2(b). As can be seen from the figure, the predicted and measured thermal conductivities agree well and are within the experimental and computational error bars for the entire range of temperature considered. Noticeably, with increasing temperature, while the particle-channel contribution decreases (as $1/T$ [5]), the coherent-channel contribution increase. As a result, the total thermal conductivity has a weaker temperature dependence than $1/T$, which is consistent with experiments [6]. This temperature dependence of thermal conductivity establishes the validity of multichannel thermal transport and is not explainable by the single-channel particlelike transport model with a $1/T$ dependence of temperature [5].

In summary, using the highest level of thermal transport theory including the effect of finite-temperature PES, lattice thermal expansion, IFC renormalization, 4-ph scattering, and the full solution of the PBTE, the validity of the recently proposed multichannel thermal transport model is tested for Tl$_3$VSe$_4$. The predicted thermal conductivity from the particlelike channel falls short of the experimental measurement by more than a factor of 3. On including the contribution from the coherent transport channel, the total thermal conductivity from multichannel transport shows a weaker than $1/T$ dependence on temperature and is in excellent agreement with experiments. This work reestablishes the importance of multichannel thermal transport in correctly capturing the thermal transport physics in strongly anharmonic solids.

[1] D. R. Clarke, Surf. Coat. Technol. **163**, 67 (2003).
[2] C. Dames and G. Chen, *Thermoelectrics Handbook: Macro to Nano* (CRC Press, Boca Raton, FL, 2005), Chap. 42, pp. 42-1–42-11.
[3] L. Lindsay, C. Hua, X. Ruan, and S. Lee, Mater. Today Phys. **7**, 106 (2018).
[4] J. M. Ziman, *Electrons and Phonons* (Oxford University Press/Clarendon, Oxford, UK, 1960).
[5] J. A. Reissland, *The Physics of Phonons* (Wiley, New York, 1973).
[6] S. Mukhopadhyay, D. S. Parker, B. C. Sales, A. A. Puretzky, M. A. McGuire, and L. Lindsay, Science **360**, 1455 (2018).
[7] A. Einstein, Ann. Phys. **340**, 679 (1911).
[8] D. G. Cahill, S. K. Watson, and R. O. Pohl, Phys. Rev. B **46**, 6131 (1992).
[9] M. Simoncelli, N. Marzari, and F. Mauri, Nat. Phys. **15**, 809 (2019).
[10] Y. Luo, X. Yang, T. Feng, J. Wang, and X. Ruan, Nat. Commun. **11**, 2554 (2020).
[11] Y. Xia, K. Pal, J. He, V. Ozoliņš, and C. Wolverton, Phys. Rev. Lett. **124**, 065901 (2020).
[12] A. J. McGaughey, A. Jain, H.-Y. Kim, and B. Fu, J. Appl. Phys. **125**, 011101 (2019).
[13] D. West and S. K. Estreicher, Phys. Rev. Lett. **96**, 115504 (2006).
[14] O. Hellman, P. Steneteg, I. A. Abrikosov, and S. I. Simak, Phys. Rev. B **87**, 104111 (2013).
[15] N. Shulumba, O. Hellman, and A. J. Minnich, Phys. Rev. B **95**, 014302 (2017).
[16] D. S. Kim, O. Hellman, J. Herriman, H. Smith, J. Lin, N. Shulumba, J. Niedziela, C. Li, D. Abernathy, and B. Fultz, Proc. Natl. Acad. Sci. USA **115**, 1992 (2018).
[17] D. C. Wallace, Phys. Rev. **152**, 247 (1966).
[18] N. K. Ravichandran and D. Broido, Phys. Rev. B **98**, 085205 (2018).
[19] M. Omini and A. Sparavigna, Phys. Rev. B **53**, 9064 (1996).
[20] D. A. Broido, A. Ward, and N. Mingo, Phys. Rev. B **72**, 014308 (2005).
[21] See Supplemental Material at http://link.aps.org/supplemental/10.1103/PhysRevB.102.201201 for details on the computational approach, parameters, convergence tests, thermal displacement, participation ratio, Grüneisen parameters, and mode-dependent phonon properties.
[22] S.-i. Tamura, Phys. Rev. B **27**, 858 (1983).
[23] J. R. Yates, X. Wang, D. Vanderbilt, and I. Souza, Phys. Rev. B **75**, 195121 (2007).
[24] W. Li, L. Lindsay, D. A. Broido, D. A. Stewart, and N. Mingo, Phys. Rev. B **86**, 174307 (2012).
[25] D. R. Hamann, Phys. Rev. B **88**, 085117 (2013).
[26] T. Feng and X. Ruan, Phys. Rev. B **97**, 045202 (2018).
[27] T. Tadano and S. Tsuneyuki, Phys. Rev. Lett. **120**, 105901 (2018).
[28] A. Jain and A. J. McGaughey, Comput. Mater. Sci. **110**, 115 (2015).
[29] P. Giannozzi, S. Baroni, N. Bonini, M. Calandra, R. Car, C. Cavazzoni, D. Ceresoli, G. L. Chiarotti, M. Cococcioni, I. Dabo, A. D. Corso, S. de Gironcoli, S. Fabris, G. Fratesi, R. Gebauer, U. Gerstmann, C. Gougoussis, A. Kokalj, M. Lazzeri,

L. Martin-Samos *et al.*, J. Phys.: Condens. Matter **21**, 395502 (2009).

[30] J. Klarbring, O. Hellman, I. A. Abrikosov, and S. I. Simak, Phys. Rev. Lett. **125**, 045701 (2020).

[31] At a temperature of 300 K, the calculated MSD of Tl atoms using bare harmonic IFCs is 4% larger when computed using the classical Boltzmann statistics compared to that with the quantum Bose-Einstein statistics.